FULL-WAVE ANALYSIS OF THE INFLUENCE OF CONDUCTOR SHAPE AND STRUCTURE DETAILS ON LOSSES IN COPLANAR WAVEGUIDE

Werner Schroeder and Ingo Wolff

Department of Electrical Engineering*
Duisburg University, D-47048 Duisburg, Germany

ABSTRACT

The influence of technological details like two-layer structure of conducting strips, layer misalignment, non-rectangular conductor shape, dielectric cover or support layers on losses in CPW with small lateral dimensions is investigated by means of the *hybrid-wave Boundary Integral Equation Method* (BIEM). A short account of recent developments in this method, as required for this investigation, is given with focus on two concepts of general interest, *the Method of Least Squares with Intermediate Projection* (MLSIP) and a *regularization approach*.

INTRODUCTION

Conductor losses play an important role in CPW based MMICs, in particular in millimeter wave designs with small lateral dimensions. If conductor thickness, strip width and strip separation are only a few multiples of skin depth, attenuation factor and effective permittivity are significantly increased.

Accurate loss prediction requires full-wave analysis in this case and consideration of finite conductor thickness and conductivity has become state of the art (e.g. [1, 2]). Nevertheless, few results are available for small lateral dimensions (e.g. [1, 3]). Most results apply to relatively wide slots, where propagation constant and attenuation are less sensitive to the details of the current distribution. There is also an obvious lack of information as to the influence of conductor shape and structure details. The present investigation compares the "generic" CPW model of Fig. 1A against more realistic models, including

(B) different conductivity of galvanic layer and base metalization,

(C) lateral misalignment of these layers,

(D) inclined edges of the galvanic layer.

Furthermore, some intentional modifications of the generic CPW structure are analyzed with respect to their effect on losses. These are

(E) rounded conductor corners (hypothetical),

(F) a lower permittivity dielectric below conductors,

(G) a dielectric cover above the slot region.

*werner@ate.uni-duisburg.de
phone: +49 203 379 3212, fax: +49 203 379 3499

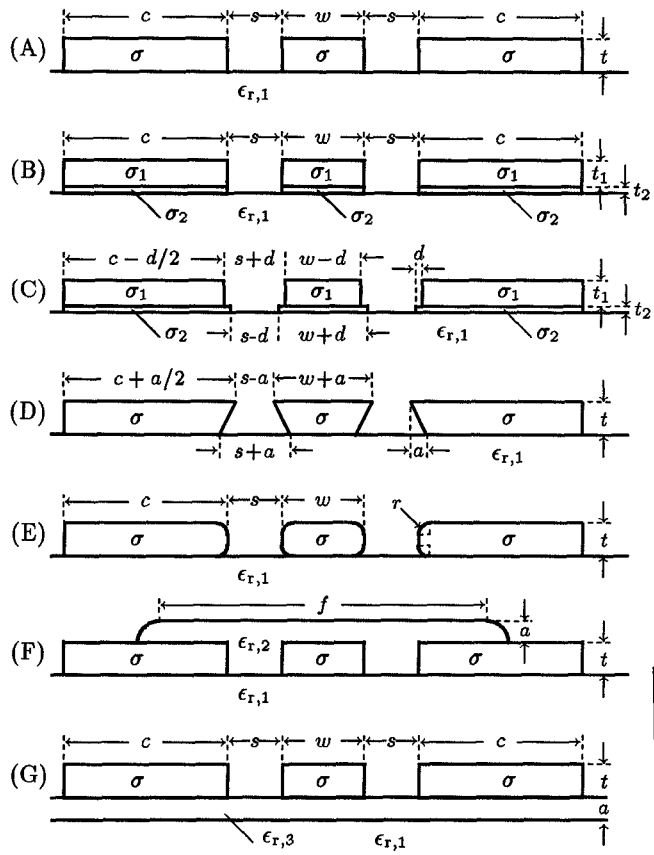

Fig. 1: Investigated CPW configurations.

Analysis of small CPW structures and in particular inclusion of the above mentioned details is a challenge for most numerical approaches, because spatial resolution must account for rapid decay of the fields within conductors, high field concentration about conductor edges and at the same time for the typically large aspect ratio of the ground planes. Domain discretization and time domain methods run to their limits in this case. The BIEM [4, 5] is an attractive alternative because it avoids domain discretization. A short account will be given of new concepts which have been introduced to extend the applicability of the BIEM to more complex geometries.

TH 3C

METHOD OF ANALYSIS

The numerical method which is applied for the present analysis is a further development in the hybrid-wave BIEM [4, 5]. The formulation is based on a system of space domain boundary integral equations

$$\mathbf{K}[a\boldsymbol{H}] - \frac{h^2}{z}\mathbf{G}[t\boldsymbol{E}] - \frac{\gamma}{z}\mathbf{G}[\frac{\partial}{\partial s}a\boldsymbol{E}] = 0, \tag{1}$$

$$\mathbf{K}[a\boldsymbol{E}] + \frac{h^2}{y}\mathbf{G}[t\boldsymbol{H}] + \frac{\gamma}{y}\mathbf{G}[\frac{\partial}{\partial s}a\boldsymbol{H}] = 0 \tag{2}$$

for the axial and transverse-tangential field components along the boundaries of each homogeneous subregion in the structure cross-section. $\mathbf{K}$ and $\mathbf{G}$ denote double layer and single layer boundary integral operators, $h \in \mathbb{C}$ is the transverse wavenumber, $z = \mathrm{j}\omega\mu$ and $y = \sigma + \mathrm{j}\omega\epsilon$. a and t represent axial and tangential unit vectors, respectively. The system of BIEs for all subregions amounts to an eigenvalue equation for the propagation constant $\gamma \in \mathbb{C}$, which also appears in the definitions of $\mathbf{K}$ and $\mathbf{G}$.

Discretization procedure

Discretization is exclusively in terms of the boundary values $a\boldsymbol{H}, t\boldsymbol{E}, a\boldsymbol{E}, t\boldsymbol{H} : \Gamma_i \rightarrow \mathbb{C}$ along subregion interfaces Γ_i. These are regular for finite conductivity with the exception of $t\boldsymbol{E}$ which becomes singular at the end of a dielectric or dielectric-air interface which connects to a corner. All regular quantities are expanded into 2^{nd}-order B-splines over an adaptive boundary partition and edge-terms with asymptotically exact singular behaviour are included for $t\boldsymbol{E}$ where required. With $\boldsymbol{U} = (u_1, \ldots, u_n)^{\mathsf{T}}$ as shorthand for the vector of expansion functions, $\boldsymbol{C} = (c_1, \ldots, c_n)^{\mathsf{T}} \in \mathbb{C}^n$ for the unknown coefficients and $\mathbf{L}(\gamma)$ for the overall BIE operator as obtained by assemblage of the couples (1), the eigenvalue equation takes the form

$$\mathbf{L}(\gamma)[\boldsymbol{U}^{\mathsf{T}}]\boldsymbol{C} = 0. \tag{3}$$

Choosing the correct approach to the discretization of the residual of the left hand side of (3) is a vital question in every projection type method. The crucial point is, that the dimension of the function space, which is occupied by the residual, in general exceeds n, because the operator is a different one for each instance of the propagation constant which is encountered in the search for eigenvalues. The Method of Moments approach to discretization with equal numbers of expansion and weighting functions is therefore insufficient and gives rise to *spurious solutions* [7]. Instead the *Method of Least Squares with Intermediate Projection* [7] is applied for the present investigation. It employs a set of weighting functions $\boldsymbol{W} = (w_1, \ldots, w_m)^{\mathsf{T}}$ with approximately twice the spatial resolution as that of $\boldsymbol{U}$, i.e. with $m \approx 2n$. As opposed to the Galerkin method, this approach yields a reliable approximation of (3) in terms of

$$\boldsymbol{W}\langle \boldsymbol{W}, \boldsymbol{W}^{\mathsf{T}}\rangle^{-1}\langle \boldsymbol{W}, \mathbf{L}(\gamma)[\boldsymbol{U}^{\mathsf{T}}]\rangle\boldsymbol{C} = \mathbf{0}. \tag{4}$$

Solutions $\gamma_i \in \mathbb{C}$ are obtained as close to zero minima of the smallest singular value of the $m \times n$ matrix

$$\langle \boldsymbol{W}, \boldsymbol{W}^{\mathsf{T}}\rangle^{-\frac{1}{2}}\langle \boldsymbol{W}, \mathbf{L}(\gamma)[\boldsymbol{U}^{\mathsf{T}}]\rangle. \tag{5}$$

Regularization

While this approach was previously applied successfully to a variety of guided wave problems it turned out that *no solutions at all* could be found for some of the *geometrically complex structures* of Fig. 1.

Because this problem is not specific to the present approach, but fundamental to integral equation formulations which amount to compact operators, we include a short account. The crucial point is, that for $n \rightarrow \infty$ equation (3), due to the *compactness* of $\mathbf{L}(\gamma)$, has an infinite set of linearly independent *approximate solutions* with arbitrarily small residual for every value of $\gamma \in \mathbb{C}$. Hence, additional restrictions on the solution space are required for finite precision calculations. Such restrictions are in fact implicitly introduced in all numerical approaches, simply by restricting the solution space to the span of the expansion functions. With an increasing number of expansion functions, however, the *regularization of the solution space*, thus introduced, tends to break down if the residual of the desired solutions is dominated by some *local approximation defect*. It may happen then, that the best approximation of the desired solution in terms of $\boldsymbol{U}$ yields higher residual than some γ-independent functions with rapid spatial variation.

This indicates that the problem is not posed in the proper solution space. Equivalently to field reconstruction from a *finite number of measurements* (as considered e.g. in microwave imaging) a *regularity condition* must be added to obtain a solution *with a finite set of weighting functions*. The theory behind this problem was recently described in more detail in [8]. It is believed, that full understanding of this problem is essential for progress in other integral

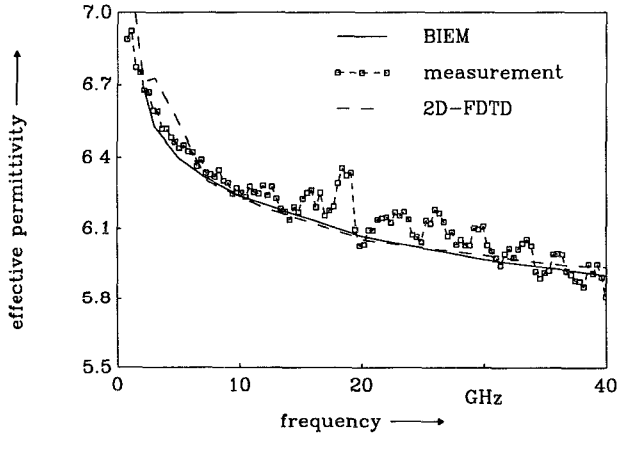

Fig. 2: Even mode effective permittivity for a CPW (Fig. 1A) with $w = 8\,\mu$m, $s = 10\,\mu$m, $c = 100\,\mu$m, $t = 3\,\mu$m, $\sigma = 22.2 \cdot 10^6$ S / m on GaAs compared to measurement [6] and 2D-FDTD simulation [3].

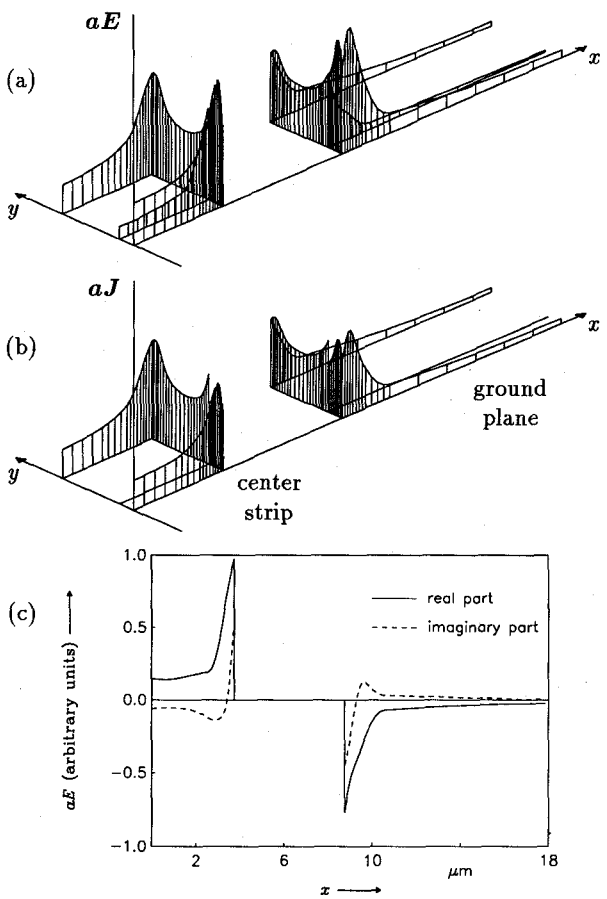

Fig. 3: Magnitude of (a) axial electric field $\boldsymbol{aE}$ and (b) axial current density $\boldsymbol{aJ}$ along conductor boundaries for configuration (B) with $p = 0.5$ at 40 GHz. Real and imaginary part of $\boldsymbol{aE}$ for $y = t_1$ are given in (c).

equation approaches also. For the present investigations a Tikhonov regularization was applied, which amounts to replacing the norm of (5) by

$$\left(\left\| \langle \boldsymbol{W}, \boldsymbol{W}^{\mathsf{T}} \rangle^{-\frac{1}{2}} \langle \boldsymbol{W}, \mathbf{L}(\gamma)[\boldsymbol{U}^{\mathsf{T}}] \rangle \right\|^2 + \left\| \mathbf{R}[\boldsymbol{U}^{\mathsf{T}}] \right\|^2 \right)^{1/2} \quad (6)$$

where $\mathbf{R}$ is an operator which adds a penalty for irregular, i.e. rapidly oscillating functions. In our context it basically measures the norm of the second derivatives of the unknown field components along subregion interfaces. Other approaches are currently under investigation.

Results

To validate the method, results have been compared against measurements and literature results, and one example is included here as Fig. 2. Results for configurations (A)–(G) of Fig. 1 are given in Figs. 3–5. The "generic" CPW (A) serves as the "origin of configuration space". In order to isolate the specific effect of each structural modification

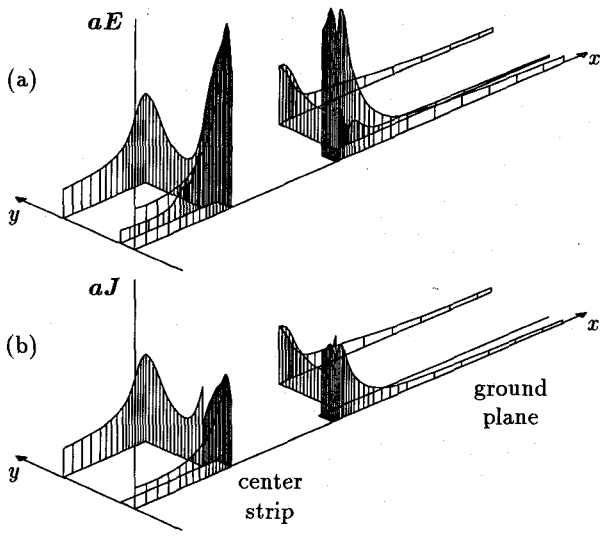

Fig. 4: Same representation as in Fig. 3 but for configuration (C) with $p = 0.5$ at 40 GHz.

in (B)–(G), most parameters are kept fixed. Moreover, average conductivity $\sigma = \sigma_1 t_1/t + \sigma_2 t_2/t = 33.33\ \mathrm{S/m}$ and total strip thickness $t = t_1 + t_2 = 3\,\mu\mathrm{m}$ are the same for all configurations, only the ratio $p = \sigma_1/\sigma_2$ is varied. An attempt is also made to maintain some "average slot width" for (B) and (C). The substrate is assumed to be lossless. It is $100\,\mu\mathrm{m}$ thick and a magnetic wall is placed below. All structures are open otherwise. The remaining dimensions are $w = 7.5\,\mu\mathrm{m}, s = 5\,\mu\mathrm{m}, c = 20\,\mu\mathrm{m}, t_1 = d = 0.6\,\mu\mathrm{m}, f = 25.5\,\mu\mathrm{m}$ and $a_i = r = 1\,\mu\mathrm{m}$. The dielectric constants are $\epsilon_{\mathrm{r},1} = 12.9, \epsilon_{\mathrm{r},2} = 3.2$ and $\epsilon_{\mathrm{r},3} = 7.3$.

With respect to loss performance, relative to configuration (A), the results for configurations (B)–(G), as given in Figs. 5a-d, can be summarized as follows:

(B) Shows no significant increase of α over that for (A) with equal average conductivity in the range $0.5 \leq p \leq 1$. The results suggest that the average conductivity approximation is permissible for loss calculations.

(C) Misalignment has a striking effect and is a most important source of additional losses. α is increased by more than 75 % at 80 GHz for $p = 0.5$, still by more than 33 % for $p = 1$.

(D) The effect in terms of attenuation per wavelength is small.

(E) Rounded corners would have some advantage. They reduce losses by approx. 10 % at 80 GHz.

(F,G) No particular merit in terms of attenuation per wavelength.

The most important conclusion addresses the technologist: precise control of base metal and galvanic layer alignment is an effective way to reduce losses. To understand the detrimental effect of lateral misalignment, it is instructive to

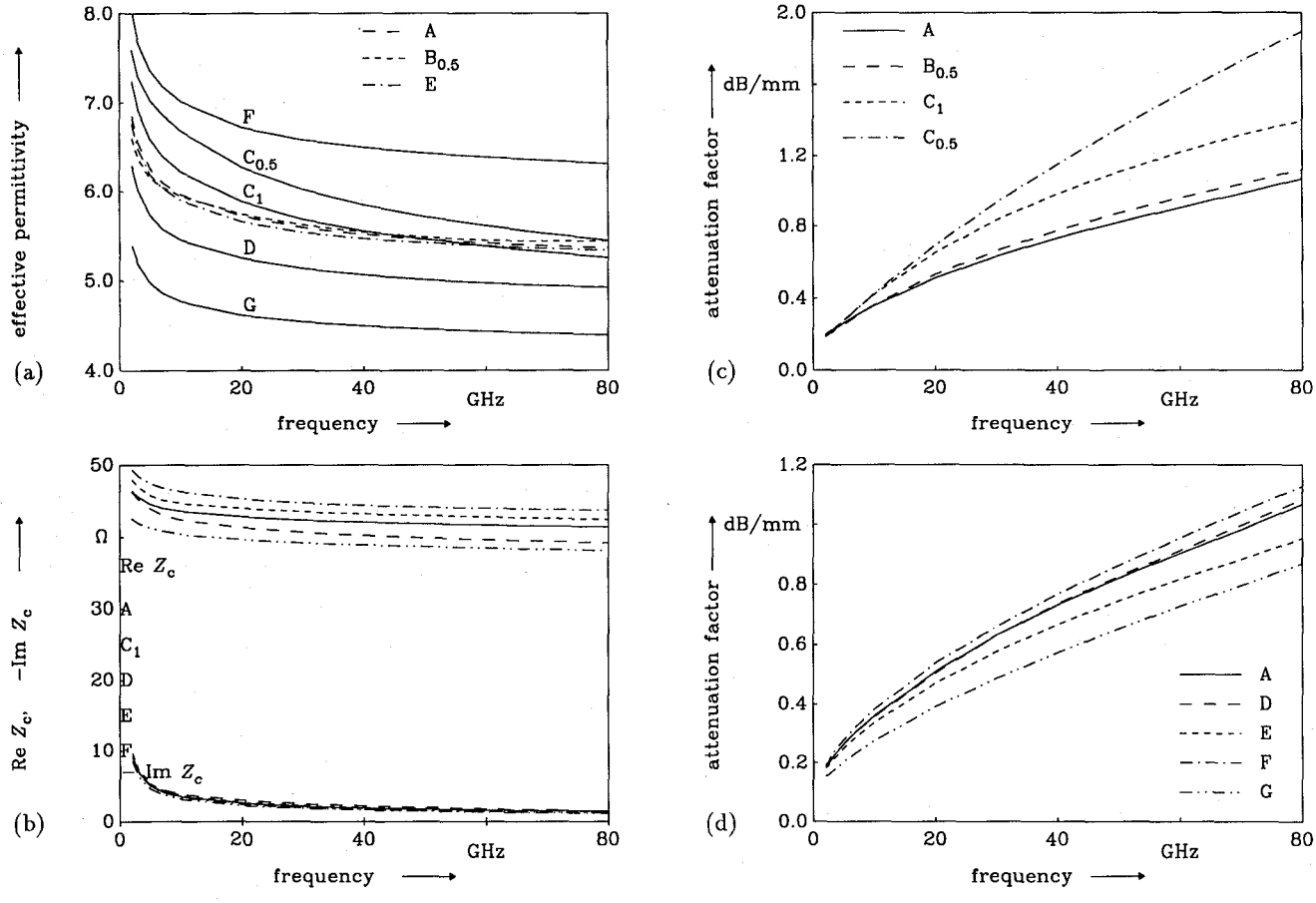

Fig. 5: (a) Effective permittivity, (b) characteristic impedance and (c,d) attenuation factor of the fundamental even mode for configurations (A)–(G) of Fig. 1. Subscripts on (B) and (C) refer to the ratio $p = \sigma_1/\sigma_2$.

compare the distributions of axial current density and axial electric field strength for configurations (B) and (C). The magnitudes of their boundary values are given in Figs. 3 and 4 over parts of the conductor contours. In configuration (C), a considerable fraction of the current concentrates in the protruding piece of the base metalization where $\boldsymbol{aE}$ is much stronger than in the rest of the strip with the consequence of large additional losses. But note that fields and currents within the conductors are complex quantities. Fig. 3c gives a plot of real and imaginary part of $\boldsymbol{aE}$ along the base metal – galvanic layer interface which clearly indicates evanescent wave propagation into the conductors.

References

[1] W. Heinrich, "Conductor loss on transmission lines in monolithic microwave and millimeter-wave integrated circuits," *Int. J. Microwave and Millimeter-Wave CAE*, vol. 2, pp. 155–167, July 1992.

[2] K. Wu, R. Vahldieck, J. L. Fikart, and H. Minkus, "The influence of finite conductor thickness and conductivity on fundamental and higher-order modes in miniature hybrid MIC's (MHMIC's) and MMIC's," *IEEE Trans. Microwave Theory Tech.*, vol. 41, pp. 421–430, Mar. 1993.

[3] S. Hofschen and I. Wolff, "Improvements of the 2-D-FDTD method for the simulation of small CPWs on GaAs using time series analysis," in *1994 IEEE MTT-S Internat. Microwave Symp. Digest*, (San Diego), pp. 39–42, May 1994.

[4] W. Schroeder and I. Wolff, "Full-wave loss analysis of normal- and superconducting transmission lines by hybrid-mode boundary integral equation method," in *1991 IEEE MTT-S Internat. Microwave Symp. Digest*, (Boston), pp. 341–344, June 1991.

[5] W. Schroeder and I. Wolff, "A hybrid-mode boundary integral equation method for normal- and superconducting transmission lines of arbitrary cross-section," *Int. J. Microwave and Millimeter-Wave CAE*, vol. 2, pp. 314–330, Oct. 1992.

[6] J. Borkes. personal communication, 1993.

[7] W. Schroeder and I. Wolff, "The origin of spurious modes in numerical solutions of electromagnetic field eigenvalue problems," *IEEE Trans. Microwave Theory Tech.*, vol. 42, pp. 644–653, Apr. 1994.

[8] W. Schroeder and I. Wolff, "On the incompleteness of integral equation formulations for electromagnetic field computations," in *Proceedings of the 24th European Microwave Conference*, vol. 1, (Cannes), pp. 567–572, Sept. 1994.